

Crossover from one- to two-dimensional space-charge-limited conduction in pentacene single crystals

Oana D. Jurchescu and Thomas T. M. Palstra^{a)}

Solid State Chemistry Laboratory, Materials Science Center, University of Groningen, Nijenborgh 4, 9747 AG Groningen, The Netherlands

(Received 31 August 2005; accepted 20 February 2006; published online 20 March 2006)

We report the crossover from one- to two-dimensional space-charge-limited conduction in pentacene single crystals with planar contacts. The space charge is confined to the in-plane longitudinal direction for $L/h \leq 15$, with L the contact separation and h the sample thickness. For $L/h > 250$ the space charge is dominated by the transverse component of the electric field. © 2006 American Institute of Physics. [DOI: 10.1063/1.2187442]

Small molecule organic crystals can exhibit large electronic mobilities at room temperature if local impurities and extended defects, such as grain boundaries, can be minimized. Thus, single crystals can provide information about the intrinsic electronic transport properties.^{1–6} Nevertheless, the evaluation of the transport parameters can be difficult because of the charge injection at the interface, or the non-uniform nature of charge carrier density, current density, and electric field under nonohmic conditions. The evaluation of the electronic mobility depends strongly on the correctness of the interdependence between electronic parameters, including mobility, charge density etc., but also on the associated geometry that is used.

In this letter, we analyze the current flow across pentacene single crystals with planar contacts. Our study focuses on the electric field E pattern for parallel planar contacts with different gap separations L . We discuss the effect of the geometric parameter L/h , with h the crystal thickness, and the anisotropy of the mobility on the electric field distribution inside the semiconductor. Effects like surface scattering, charge diffusion, surface traps,⁷ and surface polarization are neglected. We observe a gradual transition from a one- to two-dimensional (D) space-charge-limited conduction with increasing L/h . This transition has a purely geometrical origin and is determined by the distribution of the electric field inside the crystal.

The charge transport in organic conductors is often limited by the emergence of space charges. There are two limiting geometries to evaluate the conduction in the space-charge-limited current (SCLC) regime. The Mott-Gurney theory⁸ describes the current-voltage characteristics for *sandwich-type* contact geometries [Fig. 1(a)]. This is a 1D theory in which the electric field, as well as the space charge, are confined to the channel. This model gives an expression of the current density versus applied voltage:

$$J = \frac{9}{8} \Theta \epsilon_0 \epsilon_r \mu \frac{V^2}{L^3}. \quad (1)$$

Here, J is the current density for the applied voltage V , Θ is the trapping factor, L is the electrodes separation, ϵ_r is the relative dielectric constant of the material, and μ is the carrier mobility.

Geurst analyzed theoretically SCLCs in thin semiconductor layers for a *gap-structure* geometry⁹ [Fig. 1(b)]. Here, the thickness of the film is negligible with respect to the separation between the contacts. For this 2D model the longitudinal component of the electric field is responsible for the charge transport and the transversal component, perpendicular to the conduction channel, is determined by the magnitude of the space charge. His analysis leads to an expression in which the value of the current I depends quadratically on the applied voltage V , and is proportional to the relative dielectric constant of the material, ϵ_r , and inversely proportional to the square of L , the distance between the contacts:

$$I = \frac{2}{\pi} \epsilon_0 \epsilon_r \mu \frac{V^2}{L^2}. \quad (2)$$

Zuleeg *et al.*¹⁰ have introduced the width of the electrodes W , into the expression of Eq. (2). This model improves the approximation of Geurst of infinite long contact length.

Thus, the SCLC at high voltages varies with L^{-3} in the Mott-Gurney 1D theory [Eq. (1)] and with L^{-2} in Geurst 2D model [Eq. (2)]. The former was used to estimate the hole mobility in tetracene¹¹ and rubrene¹² single crystals with parallel plate electrodes. Also, it was applied for analyzing pentacene single crystals^{5,13} and tetracyanoquinodimethane (TCNQ)-coronene co-crystals¹⁴ in a *gap-type* geometry, with a conduction channel length comparable to the thickness of

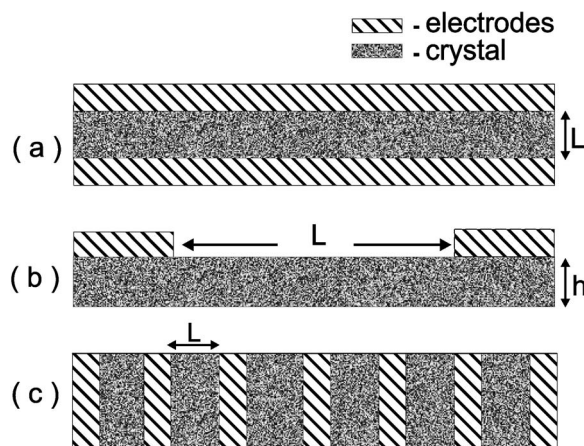


FIG. 1. Electrode configuration: (a) sandwich-type geometry—side view, (b) gap-type geometry—side view, (c) gap-type geometry—top view (used in this study).

^{a)} Author to whom correspondence should be addressed; electronic mail: t.t.m.palstra@rug.nl

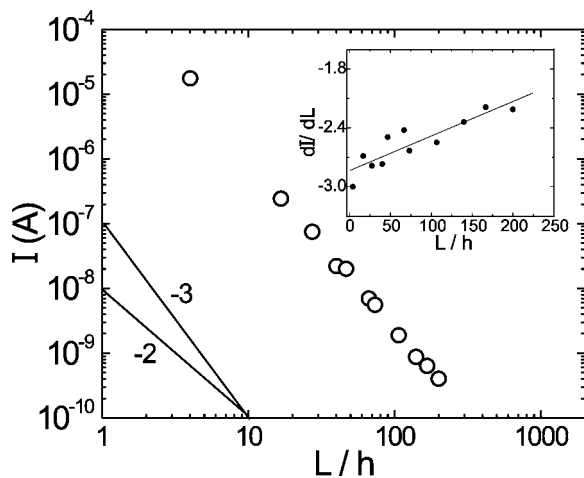


FIG. 2. Double logarithmic plot of the current at constant bias for different ratios of the planar electrode distance L with respect to the crystal thickness h . The lines are guides for the eyes and correspond to 1D model (slope -3) and 2D model (slope -2), respectively. The inset represents the derivative $d(\log I)/d(\log L)$ vs L/h . The data were obtained for one crystal with multiple contacts at room temperature.

the crystals. The model of Geurst was used to describe the charge transport of thin layers of crystalline Se,¹⁵ in which the proportionality of the current with L^{-2} was observed. The question we address, is for which parameters the 1D model can be used for planar contacts, and when the transition to the 2D model takes place. We show experimentally that for small L/h ratios, the Mott-Gurney type behavior is observed. Due to the resistivity anisotropy in different crystallographic directions and short conduction path, the current penetrates only a fraction of the crystal thickness (h_{eff}), and the electric field is homogenous. We find that for pentacene single crystals the 1D SCLC model is accurate for $L/h < 15$, whereas the 2D model applies for $L/h > 250$. The transition takes place gradually and follows the changes in the value of L/h .

Platelets of high purity pentacene single crystals were grown from double sublimation cleaned⁵ powder from Aldrich. Physical vapor transport in a horizontal glass tube under a stream of argon was used.¹⁶ The geometry of the crystals is maximally 4×4 mm in plane and thickness typically of $15\text{--}20$ μm . Pentacene crystallizes in a layered fashion and presents one morphology in the single crystal phase: with space group $P\bar{1}$.^{17,18} We painted silver epoxy contacts parallel on the crystal with a distance varying between 60 μm and 3 mm, limited by the dimensions of the crystals [Fig. 1(c)]. In this geometry, the conduction takes place predominantly along the π -stacking (c^*) direction. We used a Keithley 237 source measure unit to perform the electrical characterization. All I - V curves were taken at room temperature, in darkness and vacuum, to avoid environmental effects.¹⁹ For each single crystal of thickness h , a voltage V_{ij} was applied across a different pair of electrodes i and j attached to the sample at a distance L_{ij} and the value of the current I_{ij} was measured. The source contact was kept the same to minimize contact effects,⁷ and the drain was changed.

The I - V curves are ohmic at small biases ($I_{\Omega} \sim V$), and quadratic at high voltages ($I_{\text{SCLC}} \sim V^2$). Figure 2 shows the variation of the electrical current I at constant bias voltage for a crystal of $h = 20$ μm thickness and different contact spacings, L_{ij} (60 $\mu\text{m} < L_{ij} < 3$ mm), in the SCLC regime. The width of the contacts is approximately $W = 200$ μm . The

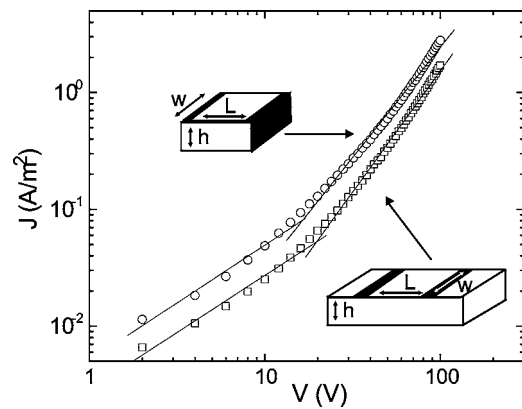


FIG. 3. Current density J vs applied voltage V for pentacene single crystal at room temperature, in vacuum and dark for gap structure contact geometry (\square), and sandwich structure configuration (\circ).

results are presented as a function of the ratio L/h . The inset shows the logarithmic derivative, $d(\log I)/d(\log L)$ vs L/h , with a value -3 corresponding to the 1D conduction, and -2 to the 2D model. As it can be observed from this graph, at small L/h ratios the bulk charges are dominant and at high ratios the surface charges determine the conduction. For $L/h \leq 15$, there is a good correspondence between the present experiment that we performed on a crystal with planar contacts and the analytical solution described by Mott-Gurney for devices with parallel plate electrodes ($I \sim L^{-3}$).⁸ This is due to the fact that at small electrode spacing L , the electric field inside the semiconductor is relatively uniform (E_{long}) and parallel to the conduction path. Moreover, when this distance is small, and considering the anisotropy of mobility in pentacene single crystals, the current is confined to the surface of the conductor.²⁰ We demonstrate that the 1D theory [Eq. (1)] has a relatively limited range of validity in case of planar parallel electrodes. It is clear from Fig. 2 that in this geometry the surface contribution becomes gradually dominant as L/h increases. The surface charge density gives rise to the normal component of the electric field (E_{trans}) and the electric field obtains more pronounced 2D characteristics. Thus the 1D space-charge approximation is not valid in this regime and the field distribution within the single crystal must be taken into account.²¹ The electric field E is no longer uniform inside the crystal. With increasing L , the transverse electric field results in $I \sim L^{-\alpha}$, with α ranging from 3 to 2 (see the inset in Fig. 2). We could not reach the $I \sim L^{-2}$ regime, corresponding to Geurst's analysis [Eq. (2)],⁹ as we were limited by the size of the crystals.

In the following we will use the SCLC technique to calculate the value of mobility in pentacene single crystals. We compare the results obtained for the mobility in the a - b plane with the two types of contact geometry described in this study. Because of different bonding and antibonding patterns, the effective mass exhibits different values for the three crystallographic directions.²² This results in a strong anisotropy of the carrier mobility, as is often observed for molecular crystals.^{1,6} This anisotropy influences the value of the L/h parameter at which the transition between 1D and 2D space charges occurs. We expect that for other molecular crystals the transition from 1D to 2D transport takes place for different geometrical parameters, due to their different mobility anisotropy.

Figure 3 shows the device configurations and current

density J versus applied bias V for one pentacene crystal within the a - b plane, using sandwich-type and gap-type architectures. The ratio $L/h=25$ in this case sets the system in the intermediate regime, where the conduction is dominated by the 1D space charges. This allows us, in first approximation, to use Eq. (1) to estimate the value of the mobility (μ) for this crystal. At low voltages, the current is ohmic. At higher voltages, the square law dependence of the current with the applied voltage is observed, corresponding to the SCLC regime. Small deviations from the linear and quadratic regimes can be attributed to the nonlinear contribution of Schottky barriers formed at the metal/pentacene interfaces. As the trap-free limit was not reached, μ cannot be determined, but only the value of the term $\Theta\mu$ can be calculated. The calculation of the mobility with sandwich configuration is straightforward. The device geometry is similar to the one of a capacitor and the electric field is constant and oriented along the direction in which the current is measured. From Eq. (1), in which the geometrical factors of the crystal are introduced ($L \times W \times h = 500 \times 200 \times 20 \mu\text{m}$), a value of $(\Theta\mu)_{\text{sandwich}} = 12 \text{ cm}^2/\text{V s}$ is obtained. In the case of gap-type structure, we can see from Fig. 2 that, as $L/h > 15$, the electric field will exhibit deviations from the idealized 1D form, and the use of simple Mott-Gurney theory is not valid. Moreover, it underestimates the value of the mobility: $(\Theta\mu)_{\text{gap}} = 7.2 \text{ cm}^2/\text{V s}$. This comes from the fact that the current flow is not homogenous distributed along the entire thickness of the crystal (h), but it is confined to the surface due to the anisotropy of pentacene. We use the Montgomery method²⁰ to determine the effective thickness (h_{eff}) penetrated by the electric field lines in this configuration. The input for this algorithm are the values of the components of the resistivity tensor along the three crystallographic directions (a, b in-plane and c^* perpendicular to the plane: $\rho_a = 1.3 \times 10^6 \Omega \text{ m}$, $\rho_b = 4.7 \times 10^5 \Omega \text{ m}$, $\rho_{c^*} = 2.1 \times 10^8 \Omega \text{ m}$), and their correspondent electrodes separation on the crystal (x, y, z). We transform this anisotropic solid into the equivalent isotropic system of dimensions x', y', z' , using van der Pauw's expression:²³

$$\frac{z_{\text{eff}}}{(xy)^{1/2}} = \frac{(\rho_a \rho_b)^{1/4}}{\rho_{c^*}^{1/2}} \frac{z'_{\text{eff}}}{(x'y')^{1/2}}. \quad (3)$$

Here z_{eff} and z'_{eff} are the effective thickness for the anisotropic and isotropic system, respectively. The second factor of the expression is the normalized effective thickness in the isotropic material, which is the abscissa of the graph proposed by Montgomery (Fig. 2 in Ref. 20). The normalized sample thickness in the isotropic space can be calculated from

$$\frac{z'}{(x'y')^{1/2}} = \frac{\rho_{c^*}^{1/2}}{(\rho_a \rho_b)^{1/4}} \frac{z}{(xy)^{1/2}} = 1.036. \quad (4)$$

The effective thickness depends on the ration x/z , in the anisotropic pentacene single crystal [Eqs. (4) and (5)], which corresponds to the order parameter L/h that we have used. Different curves are obtained for different ratios of the in-plane directions. For this particular geometry,

$$\frac{y'}{x'} = \left(\frac{\rho_b}{\rho_a} \right)^{1/2} \frac{y}{x} = 0.24. \quad (5)$$

Thus, the normalized effective thickness of this system is 0.715. This leads to the value of $z_{\text{eff}} = 0.33z$, corresponding to $h_{\text{eff}} = 0.33h$. From Eq. (1), the value of $(\Theta\mu)_{\text{gap}, h_{\text{eff}}} = 20 \text{ cm}^2/\text{V s}$ can be calculated.²⁰ This value should be considered an overestimate of the mobility. This arises mainly from the fact that in this regime small deviations appear from the 1D model that was assumed in the calculations. While the Mott-Gurney theory gives $I \sim L^{-3}$, for our L/h ratio of 25, we should have used $I \sim L^{-2.7}$ as a better approximation. In the regime $L/h \leq 15$, where the current varies with the cube of the contact separation (Fig. 2), the values of mobility obtained with the two geometries agree well.⁵ The effective thickness that we obtain represents an upper limit. Montgomery's theory assumes ohmic conduction in which the equipotential lines are independent of the magnitude of the electric field, while in the SLCL regime the current density capacity increases quadratically with the field, leading to a smaller effective penetration depth.

In conclusion, we report the crossover from 1D to 2D type SCLC conduction in pentacene single crystals with increasing L/h for gap-type contact geometry. For $L/h < 15$ the gap-type contact is well approximated by 1D space charges, whereas for $L/h > 15$ 2D space charges should be taken into account. The 1D space charges are predominant in pentacene because of the anisotropy in resistivity.

¹V. Podzorov, E. Menard, A. Borissov, V. Kiryukhin, J. A. Rogers, and M. E. Gershenson, Phys. Rev. Lett. **93**, 086602 (2004).

²D. V. Lang, X. Chi, T. Siegrist, A. M. Sergent, and A. P. Ramirez, Phys. Rev. Lett. **93**, 086802 (2004).

³C. Goldmann, S. Haas, C. Krellner, K. P. Pernstich, D. J. Gundlach, and B. Batlogg, J. Appl. Phys. **96**, 2080 (2004).

⁴D. A. da Silva Filho, E. G. Kim, and J. L. Brédas, Adv. Mater. (Weinheim, Ger.) **17**, 1072 (2005).

⁵O. D. Jurchescu, J. Baas, and T. T. M. Palstra, Appl. Phys. Lett. **84**, 3061 (2004).

⁶V. C. Sundar, J. Zaumseil, V. Podzorov, E. Menard, R. L. Willett, T. Someya, M. E. Gershenson, and J. A. Rogers, Science **303**, 1644 (2004).

⁷R. W. I. de Boer and A. F. Morpurgo, Phys. Rev. B **72**, 073207 (2005).

⁸N. F. Mott and R. W. Gurney, in *Electronic Processes in Ionic Crystals*, 2nd ed. (Clarendon, Oxford, 1948), p. 172.

⁹J. A. Geurst, Phys. Status Solidi **15**, 107 (1966).

¹⁰R. Zuleeg and P. Knoll, Appl. Phys. Lett. **11**, 183 (1967).

¹¹R. W. I. de Boer, M. Jochemsen, T. M. Klapwijk, A. F. Morpurgo, J. Niemax, A. K. Tripathi, and J. Pflaum, J. Appl. Phys. **95**, 1196 (2004).

¹²V. Podzorov, S. E. Sysoev, E. Loginova, V. M. Pudalov, and M. E. Gershenson, Appl. Phys. Lett. **83**, 3504 (2003).

¹³C. C. Mattheus, A. B. Dros, J. Baas, G. T. Oostergetel, A. Meetsma, J. L. de Boer, and T. T. M. Palstra, Synth. Met. **138**, 475 (2003).

¹⁴X. Chi, C. Besnard, V. K. Thorsmolle, V. Y. Butko, A. J. Taylor, T. Siegrist, and A. P. Ramirez, Chem. Mater. **16**, 5751 (2005).

¹⁵M. Polke, J. Stuke, and E. Vinaricky, Phys. Status Solidi **3**, 1885 (1963).

¹⁶A. Laudise, C. Kloc, P. Simpkins, and T. Siegrist, J. Cryst. Growth **187**, 449 (1998).

¹⁷C. C. Mattheus, A. B. Dros, J. Baas, A. Meetsma, J. L. de Boer, and T. T. M. Palstra, Acta Crystallogr. **57**, 939 (2003).

¹⁸C. C. Mattheus, G. A. de Wijs, R. A. de Groot, and T. T. M. Palstra, J. Am. Chem. Soc. **125**, 6323 (2003).

¹⁹O. D. Jurchescu, J. Baas, and T. T. M. Palstra, Appl. Phys. Lett. **87**, 052102 (2005).

²⁰H. C. Montgomery, J. Appl. Phys. **42**, 2971 (1971).

²¹S. Hirota, J. Appl. Phys. **50**, 3003 (1979).

²²G. A. de Wijs, C. C. Mattheus, R. A. de Groot, and T. T. M. Palstra, Synth. Met. **139**, 109 (2003).

²³L. J. van der Pauw, Philips Res. Rep. **16**, 187 (1961).